Current THD comparison of different offset injections in the linear modulation range for cascaded H-bridge converters

Mohammad Umar Khan
School of Engineering
Liverpool John Moores University
Liverpool, UK
m.u.khan@2017.ljmu.ac.uk

Obrad Dordevic
School of Engineering
Liverpool John Moores University
Liverpool, UK
o.dordevic@ljmu.ac.uk

Martin Jones
School of Engineering
Liverpool John Moores University
Liverpool, UK
m.jones2@ljmu.ac.uk

Abstract—The equivalence of space vector pulse width modulation (PWM) and carrier-based PWM through the injection of a common-mode voltage is already known for two-level (first min-max injection) and multilevel (double min-max injection) three-phase converters. However, under regular sampled phase voltage references, these injections do not produce the lowest total harmonic distortion (THD) of the load phase current throughout the linear modulation index range. This paper proposes the use of a similar common-mode injection, called the second min-max injection that achieves the lowest current THD in regions of the modulation index range where the double min-max injection fails to do so. A cascaded H-bridge (CHB) topology is analyzed, and comparison is made between different multicarrier modulation strategies, using simulation results, under different injections for the whole modulation index range. The level-shifted in-phase disposition modulation method is found to produce the lowest load phase current THD with second min-max offset voltage injection for modulation indices below unity. For modulation indices greater than one, the double min-max injection is still considered as optimal.

Keywords—Multilevel converters, multilevel inverters, cascaded H-bridge (CHB), zero-sequence, offset, common-mode injection, min-max injection, double min-max injection

I. INTRODUCTION

Development of the multilevel converter is a prominent technology for high-power conversion. Compared to the two-level converter, multilevel converters benefit from features such as low total harmonic distortion (THD), better harmonic profile, reduced dv/dt, smaller passive filters, lower switching frequency (losses), smaller common mode voltages, and the possibility to use lower rated semiconductor devices [1].

Various ingenious arrangements of switching devices, called converter topologies, have been researched and commercialized for different industrial applications in power distribution, renewable energy systems, and variable frequency drives. The neutral point clamped (NPC), flying capacitor (FC) and cascaded H-bridge (CHB) converters are commonly classified as the three classic multilevel converter topologies [1]. Several variants of the NPC converter and other hybrid multilevel converter topologies have been reported in the literature with application specific relevance [2]. A series connection of multiple modular converter units can be further classified as cascaded multilevel converters [3]. Although many different topologies can be cascaded, a cascaded connection of full bridge (H-bridge) modules in a CHB and that of half-bridge modules (cells) in the modular multilevel converter (MMC) have proven to be the most popular options [4].

The cascaded H-bridge multilevel converter has found use in a variety of applications such as in variable frequency motor drive systems, flexible ac transmission systems for reactive power compensation, utility interface for renewable energy sources, and for traction applications [2]–[5]. The CHB converter requires the least number of components for the same number of output levels when compared to other classic multilevel topologies [6]. Moreover, the CHB converter has been shown to be the most suitable for fault-tolerant operation among the classic multilevel converter topologies [7]. Additionally, superior reliability of the CHB has been reported, compared to the MMC, under equivalent operating conditions and redundancies in a three-phase drive application [8]. Furthermore, the CHB performs favorably compared to other topologies such as the NPC and MMC converters for motor drive application in terms of efficiency [9], [10].

Numerous modulation and control strategies are applicable to the CHB converter. These can be classified based on the switching frequency. For low/fundamental switching frequencies, multilevel selective harmonic elimination (SHE) and nearest level modulation (NLM) are the primary modulation methods that serve applications demanding lower switching losses [11]. For high switching frequencies, carrier-based PWM including the phase-shifted PWM is the most recommended modulation method due to its natural capacity for balanced dc-link utilization and loss equalization [2], [5]. Level-shifted multicarrier PWM methods are also applicable to the CHB but require additional power equalization strategy for full effectiveness [11]. The space vector PWM (SVPWM) is another high frequency modulation method that is beneficial, but its implementation entails increasingly complex calculations with an increase in the number of converter levels and phases.

The relationship between space vector PWM and regular sampled PWM for two-level converters had been established in the early 1990s [12]. Later, the equivalence between the sine-triangle PWM and SVPWM technique was demonstrated through double min-max injection for multilevel converters [13]–[15]. However, the proposed method was analyzed only for certain modulation index values and the effect on the phase current THD was not studied.

The output voltage imbalance in multilevel CHB converters has been addressed [16] using weighted min-max zero sequence injection for electric vehicle application using phase-shifted PWM, which is known to produce suboptimal harmonic performance compared to the level-shifted PWM. Similarly, zero sequence injection has been studied for solving voltage imbalance conditions in CHB converters for grid-

photovoltaic integration using the weighted min-max zero sequence injection [17], optimized third harmonic injection [18], double third harmonic, and double min-max injection [19].

The carrier-based in-phase disposition PWM method was demonstrated to be equivalent to the space vector PWM scheme with double min-max injection for three-level five phase NPC converter [20]. Experimental verification confirmed equivalent performance in terms of the phase voltage and current harmonic distortion over a wide modulation index range but with a significantly higher computational cost incurred by the space-vector method. Although the study considered a three-level NPC converter, its validity for a higher-level CHB converter demands further examination.

Recently, several iterations of carrier-based techniques, equivalent to the SVPWM, based on different zero sequence injections were proposed for different combinations of multilevel multiphase systems for purposes such as switching loss minimization and common mode voltage reduction [21]. The carrier-based double min-max zero sequence injection was also discussed as being equivalent to SVPWM by producing centrally spaced active voltage vectors. Experimental verification of the proposed methods on a five-level CHB converter showed significantly lower resource usage with the carrier-based implementation for different zero sequence injections compared to the space vector PWM. The authors did not, however, investigate the distinction between the harmonic distortion profiles for different modulation methods over a wide range of modulation indices.

Although the first and double min-max injections have been proposed and studied in the literature, limited literature is available on the harmonic performance of different carrier-based modulation strategies with appropriate zero sequence injections for a wide modulation index range for a CHB converter. To the authors' knowledge, no study has been conducted to confirm superior load current THD performance of (only) the second min-max injection under certain modulation indices for a regular sampled phase voltage reference waveform. In this paper, comparison is made between carrier-based phase-shifted and level-shifted modulation methods, under different min-max injections, in terms of the harmonic distortion of the load phase current generated by a three-phase multilevel CHB converter over a wide modulation index range.

The paper is organized as follows. Section II provides a brief description of a three-phase cascaded H-bridge multilevel converter. In Section III, multicarrier phase- and level-shifted modulation schemes are discussed. The issue of uneven distribution of power between different modules of a CHB under level-shifted schemes is also addressed. After that, different types of offset voltage injections for a multilevel converter are described in section IV. The simulation results for the proposed offset injections are presented and discussed in section V. Finally, a conclusion is provided in section VI.

II. CASCADED H-BRIDGE CONVERTER

A cascaded connection of several H-bridge modules results in the synthesis of an output voltage waveform, which is the sum of all module outputs. The considered case, shown in Fig. 1, is where all dc sources have identical voltages (symmetric configuration) and each module can generate three voltage levels ($+V_{\mathrm{dc}}$, 0, and $-V_{\mathrm{dc}}$) depending on the

switching state combination. The output leg voltage waveform of a CHB converter is made up of $l = 2k + 1$ voltage levels, where k is the number of H-bridge modules per leg, each with its own isolated dc source, depicted by a battery in Fig. 1(b). A general formula for the leg voltages of a three-phase symmetric CHB converter consisting of k modules per converter leg can be given by:

$$v_{xn} = \sum_{i=1}^{k} v_{xi} \qquad (1)$$

where x can be any of three phases (a, b, or c). For a balanced three-phase system, the potential difference between the load neutral point s and inverter neutral point n, called the offset (also known as common-mode or zero sequence) voltage, can be defined as the average of the converter leg voltages:

$$v_{sn} = (v_{an} + v_{bn} + v_{cn})/3 \qquad (2)$$

Similarly, the load phase voltages, which sum up to zero, are given as:

$$\begin{cases} v_{as} = v_{an} - v_{sn} = \dfrac{1}{3}(v_{ab} - v_{ca}) \\[2mm] v_{bs} = v_{bn} - v_{sn} = \dfrac{1}{3}(v_{bc} - v_{ab}) \\[2mm] v_{cs} = v_{cn} - v_{sn} = \dfrac{1}{3}(v_{ca} - v_{bc}) \end{cases} \qquad (3)$$

As a point of pertinence, the offset voltage can be observed to have been cancelled from the phase voltages (3). The load phase currents in a star-connected balanced three-phase system sum up to zero and are related to the phase voltages for any of the three phases: $x = (a, b,$ or $c)$, as:

$$v_{xs} = Ri_x + L\frac{di_x}{dt} \qquad (4)$$

III. MULTICARRIER PULSE WIDTH MODULATION

Carrier-based PWM methods are implemented by comparing high frequency triangular carriers with the desired reference (modulating) waveform to generate switching pulses. Pulse widths are determined by the intersection of the reference and carrier waves. The objective of any PWM technique is to produce phase voltages as close as possible to the desired sinusoidal voltage waveform. However, in the case of a three-phase system, the converter output voltage is the leg voltage, which is compared with high frequency carriers to obtain the gating signals for the switching devices in each module of a CHB converter. The carrier waveforms can be either in the shape of a sawtooth or a triangular shape. A triangular shaped carrier is known to produce better harmonic results and is nowadays generally accepted as the standard carrier waveform.

Naturally sampled PWM is popular due to its simple implementation with analog circuits. However, its digital implementation can be complicated and resource heavy for microcontrollers. Instead, regular sampled symmetric or asymmetric reference waveforms can be used to make performance gains with minimal loss in performance provided a sufficiently high sampling (carrier) frequency is used. It has been established that symmetric sampling returns a poorer harmonic performance, compared to asymmetric sampling, with a large second order harmonic component, incomplete cancellation of the sideband harmonics around odd multiples
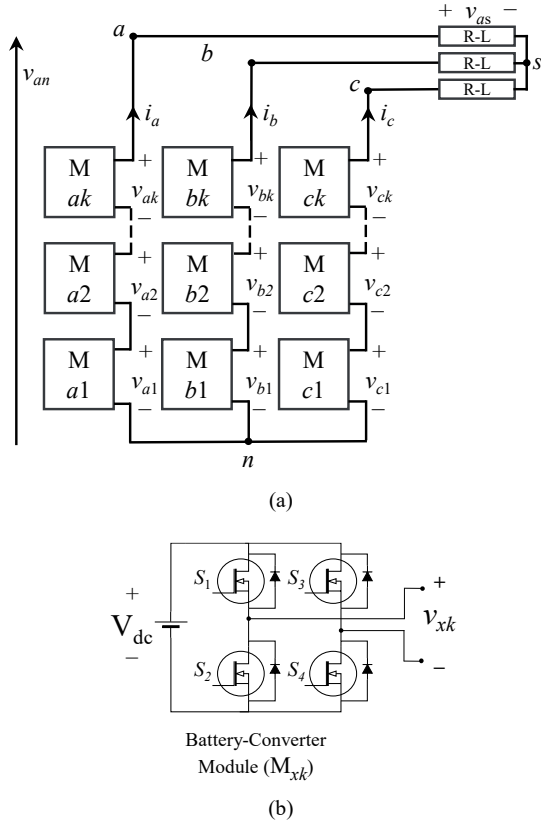
(a)

Battery-Converter
Module (M$_{xk}$)

(b)

Fig. 1 (a) Configuration of a three-phase k module cascaded H-bridge converter connected to a three-phase RL load (b) a battery-converter module

of the carrier frequency in the output, and consequently should not be considered for implementation [15].

To proceed with the description of the modulation methods, the definition of the modulation index for a CHB multilevel converter is necessary:

$$m = \frac{\tilde{V}_{xs}}{kV_{dc}} \quad (5)$$

where V_{dc} is the dc-link voltage across one H-bridge module in each converter leg, and $\tilde{V}_{xs}$ is the amplitude of the reference phase voltage for phase a, b, or c, which can be defined as:

$$\tilde{v}_{xs} = \tilde{V}_{xs} \cdot \sin(\omega_r t + \phi) = m \, kV_{dc} \cdot \sin(\omega_r t + \phi) \quad (6)$$

where ϕ is 0, $-2\pi/3$, and$-4\pi/3$ for the three phases a, b, and c respectively, and $\omega_r = 2\pi f_r$ is the fundamental angular frequency of the reference waveforms. The phase reference voltages can be normalized with respect to V_{dc} for simplification in calculation of the switching signals and for implementation of different offset voltage injections:

$$\hat{v}_{xs} = m \cdot k \cdot \sin(\omega_r t + \phi) \quad (7)$$

A. Multicarrier Phase-shifted PWM

Multicarrier phase-shifted (PS) PWM for a cascaded H-bridge is an extension of the unipolar phase-shift modulation method for two-level converters. For a CHB with k modules per leg, a pair of triangular carriers, which are 180° out of phase with each other, are required per module – one for each H-bridge leg. The amplitude of the normalized carrier waveforms should be the same as the number of modules k to

satisfy definition of the modulation index in (5). Therefore, the total number of triangular carriers required for a CHB is $2k$. The phase shift between any two adjacent carriers should be 180°/k. For example, a CHB with 4 H-bridge modules ($k = 4$) would require 8 triangular carriers with a phase shift of 45° between any two adjacent carriers. Even at low modulation indices, all H-bridges would still be utilized equally as the reference wave is intersected by all the carrier waveforms. The switching frequency of the devices in PS-PWM equals that of the carrier frequency.

B. Multicarrier Level-shifted PWM

Multicarrier level-shifted (LS) PWM schemes differ in the vertical disposition of the carrier waves and the phase relationship between adjacent carriers. The three possible level-shifted PWM schemes are:

- *In-phase disposition* (IPD): vertically level-shifted multiple carriers such that all carriers are in phase with each other.
- *Phase opposition disposition* (POD): carriers in the positive region are in phase with each other but are 180° out of phase with those in the negative region.
- *Alternate phase opposition disposition* (APOD): adjacent carrier waves are phase-shifted by 180° and can be said to be alternatively in phase opposition.

The amplitude of the normalized carrier waveforms should be 0.5 to satisfy the modulation index defined in (5). The total number of triangular carrier waveforms required remains the same at $2k$ carriers. The switching frequency of the converter for all level-shifted PWM schemes equals that of the carrier frequency with unequal switching frequency of devices in different H-bridge modules. The average device switching frequency for LS-PWM is $f_c/(2k)$. This necessitates appropriate choice of the carrier frequency for fair comparison between the level- and phase-shifted methods. The carrier frequency for the LS-PWM schemes can be chosen as $2k$ times that of the PS-PWM for equivalence between the average device switching frequencies of both methods.

C. Equal Power Distribution

The advantage of the multicarrier phase-shifted (PS-PWM) is the equal utilization of dc sources. On the contrary, level-shifted modulation methods suffer from unequal device conduction times and switching frequencies for each of the H-bridge modules, leading to unequal utilization of dc sources in a CHB converter. The vertical distribution of the carriers at different voltage levels allows partial or no intersections between the reference and carrier waveforms depending on the modulation index. This can be mitigated through the cyclical rotation of the carrier waveforms to occupy different voltage levels sequentially at different times. A simple implementation is shown in Fig. 2 where the voltage contribution of each H-bridge in the CHB is sequentially equalized over two fundamental cycles.

IV. OFFSET VOLTAGE INJECTION

The maximum linear modulation index in the case of sinusoidal PWM is limited to unity, which can be further extended by appropriate offset voltage injection to a maximum of 1.1547 ($2/\sqrt{3}$). One such offset voltage injection
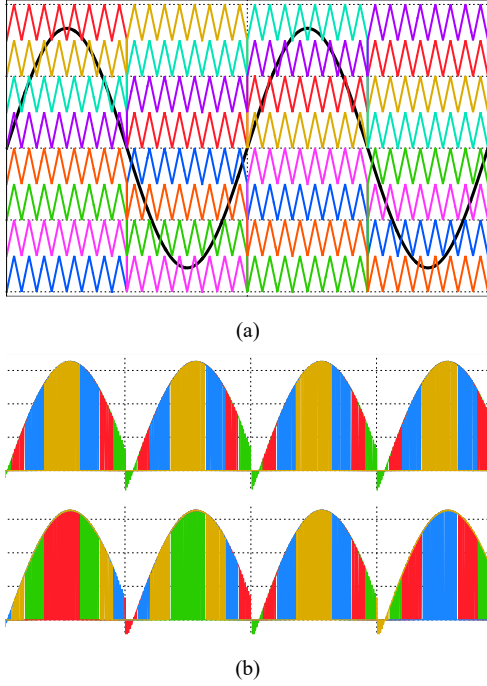
Fig. 2 (a) Equal power distribution through cyclic rotation of the carriers (b) All dc-souce battery currents showing unequal utlization under LS-PWM (top) and after carrying out cyclic rotation shown in (a) – bottom subplot.

is the well-known third harmonic injection (THI) of one-sixth amplitude found in literature for the two-level converter, whereas one-quarter magnitude THI is also possible, which reduces the THD at the cost of slightly reduced maximum linear modulation index range [22]. THI is also applicable to the CHB converter for increasing the modulation index range.

The cancellation of the offset voltage in the line and phase voltages of a three-phase system allows for utilization of a suitable common-mode injection. The underlying relationship between the required leg voltage, the desired phase voltage and the offset voltage can be given as:

$$\hat{v}_{xn} = \hat{v}_{xs} + \hat{v}_{sn} \qquad (8)$$

Consequently, the reference phase voltages can be set as the desired sinusoid and any appropriate (within linear modulation range) offset voltage can be added to obtain the required leg voltage waveform for comparison with the carrier signals.

A. Sinusoidal Reference (00)

In the case of sinusoidal PWM, the desired phase voltage reference is taken as the converter leg voltage reference for comparison with the carriers. Accordingly, no offset voltage is added to the phase voltage, thus:

$$\hat{v}_{sn} = 0 \qquad (9)$$

Consequently, from (8) the leg voltage equals the desired phase voltage:

$$v_{xn}^{00} = \hat{v}_{xs} \qquad (10)$$

B. First Min-max Injection (10)

Likewise, it has been shown that the subtraction of the instantaneous average of the maximum and minimum values of the reference phase voltages from each reference phase

voltage results in the centering of each reference leg voltage within the modulation period [14]. The offset voltage for the first min-max injection can be defined as:

$$v_{sn}^{10} = -(\min(\hat{v}_{xs}) + \max(\hat{v}_{xs}))/2 \qquad (11)$$

where $x = (a, b,$ and $c)$. The resulting leg voltage with the first min-max injection becomes:

$$v_{xn}^{10} = \hat{v}_{xs} + v_{sn}^{10} \qquad (12)$$

The first offset injection to the three-phase references results in the centering of the active space vectors within a switching period for the two-level converters [15]. In addition to the increase in the dc voltage utilization to 1.1547, the first min-max injection results in the lowering of the total harmonic distortion of the phase current [22]. However, it is not the most effective strategy for lowering the total harmonic distortion of the phase current for multilevel converters, as will be shown.

C. Double Min-max Injection (11)

The equivalence between SVPWM and IPD-PWM was established with the double min-max injection for the multilevel CHB [13]. It has been shown that the centering of the active space vectors achieved by the first injection is not adequate for multilevel converters as only the vectors of odd redundancy are centered on either side of the half switching period [13]. This is because references in a multilevel waveform lie at different voltage levels occupied by different carrier waveforms. It cannot be guaranteed that the references with the maximum and minimum values will be responsible for producing the first and the last switching transitions, i.e., the active voltage vector sequence cannot be determined. Therefore, after the application of the first min-max injection, the normalized reference leg voltage waveforms are brought to a common voltage level within the same carrier level using the modulus function as:

$$\acute{v}_{sn}^{11} = \mathrm{mod}\left(k + v_{xn}^{10}, \frac{2k}{l-1}\right) \qquad (13)$$

where normalization with respect to V_{dc} leads to the term $2k/(l-1)$ being equal to 1. A dc offset of k is also added, as a precaution to avoid unexpected results from the modulus operation on negative values. This allows for the min-max calculation of a new offset voltage and subsequent re-application of min-max injection that results in achieving the double min-max injection (v_{sn}^{11}):

$$v_{sn}^{11} = v_{sn}^{10} + \frac{k}{l-1} - \frac{(\min(\acute{v}_{sn}^{11}) + \max(\acute{v}_{sn}^{11}))}{2} \qquad (14)$$

The leg voltage reference resulting from double min-max injection thus becomes:

$$v_{xn}^{11} = \hat{v}_{xs} + v_{sn}^{11} \qquad (15)$$

This achieves equalization of the first and the last voltage vectors while centering the active space vectors within the carrier period [22].

D. Second Min-max Injection (01)

Double min-max injection applies the first offset voltage injection prior to the application of the modulus function to bring the reference waveform into a common carrier level. Instead, by first bringing multilevel reference waveforms into a common carrier interval, and only then calculating and applying the offset voltage produces reference waveforms with centered active voltage vectors and with equally spaced

zero vectors at the beginning and the end of the carrier interval. Therefore, the normalized offset voltage for *only* the second injection (v_{sn}^{10}) can be defined as:

$$\acute{v}_{sn}^{01} = \mathrm{mod}\left(k + \hat{v}_{xs} \, , \, \frac{2k}{l-1}\right) \qquad (16)$$

$$v_{sn}^{01} = \frac{k}{l-1} - \frac{(\min(\acute{v}_{sn}^{01}) + \max(\acute{v}_{sn}^{01}))}{2} \qquad (17)$$

Likewise, the reference leg voltage after the second (only) injection becomes:

$$v_{xn}^{01} = \hat{v}_{xs} + v_{sn}^{01} \qquad (18)$$

The second min-max injection, however, does not lead to an increase in the modulation index range. This is because the first min-max injection calculates the required offset voltage from the desired phase voltage references ($\hat{v}_{xs}$) for re-injection into the phase voltage references. However, when the second min-max injection is performed, the first min-max injection term is not included.

V. SIMULATION RESULTS

The modeling and simulation of the complete system was carried out in PLECS. A three-phase cascaded H-bridge converter with $k = 4$ modules per leg was developed in a symmetrical configuration with $V_{dc} = 30\,\mathrm{V}$, with a peak leg voltage of $120\,\mathrm{V}$, using ideal switches (with V_{on} and R_{on} taken as zero). For simplicity, dead time was not implemented. The converter was connected to a balanced three-phase RL load in star configuration with $R = 10\,\Omega$ and $L = 20\,\mathrm{mH}$. Three-phase balanced sinusoidal phase voltages with a fundamental frequency of 50 Hz were used as reference waveforms with a variable amplitude as per definition of modulation index in (5). The references were regular sampled asymmetrically and were then subjected to the min-max strategies proposed in section IV. The system simulation was carried out for PS, IPD, POD, and APOD PWM methods with each injection under an equivalent switching frequency of 1 kHz per H-bridge module. The total harmonic distortion (THD) for leg and phase voltages, and phase currents was calculated using the formula:

$$\mathrm{THD}_U = \sqrt{\frac{U_{rms}^2 - U_0^2 - U_1^2}{U_1^2}} \times 100\% \qquad (19)$$

where U stands for either the leg voltage, phase voltage, or the phase current. The simulation was allowed to fully settle into a steady state condition before obtaining the THD data.

In Fig. 3, multicarrier PWM methods were compared to each other in terms of the total harmonic distortion of the phase current waveforms over the entire linear modulation index range for all the injections described in section IV. It is obvious that IPD-PWM produces the lowest phase current THD among all the multicarrier modulation methods for all analyzed injections. Similarly, IPD-PWM generates the lowest phase voltage THD profile (not shown) between these modulation methods for the whole modulation index range. Therefore, further on only IPD-PWM is analyzed.

The phase current THD profiles for IPD-PWM under different injections in Fig. 4 show that the second min-max injection produces the best current THD profile for $m \leq 1$. The second min-max injection is not valid for $m > 1$, and double min-max injection produces a lower current THD in the extended modulation range compared to the first min-max
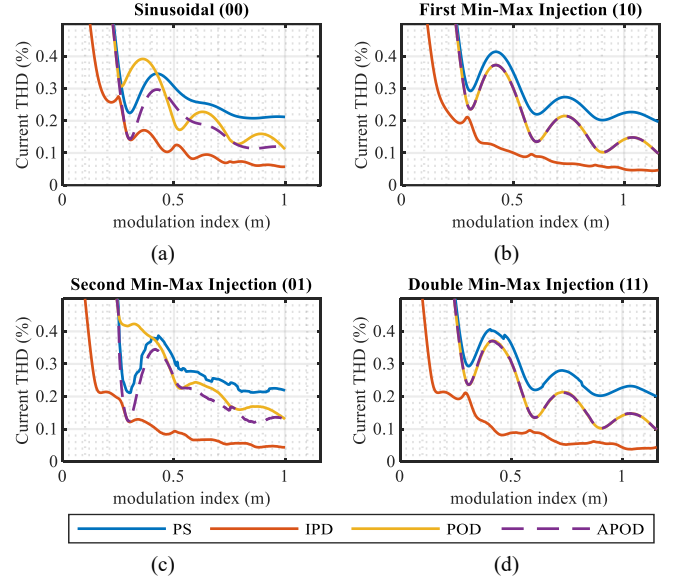

Fig. 3 Phase current THD (%) profiles for phase- and level-shifted modulation methods under different reference waveforms: (a) sinusoidal (00), (b) first min-max injection (10), (c) second min-max injection (01), and (d) double min-max injection (11).
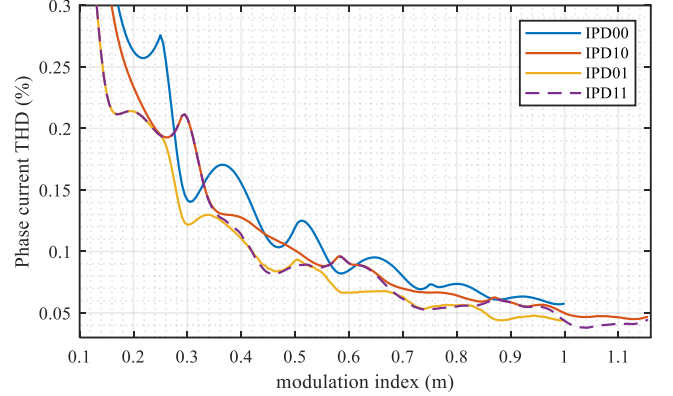

Fig. 4 Phase current THD (%) profiles for in-phase disposition (IPD) modulation method for different injections.

injection. It can be noticed that both the second and double injections produce practically identical current THD for $m \leq 0.25$, which is where only one battery-converter module is activated (three-level waveform operation). Other such regions of similar distortion are also present at higher modulation indices. However, the second min-max injection consistently produces the lowest current THD below unity modulation index.

An operating point where the current THD difference between the double and second (only) injection is the largest is found to be at $m = 0.3$. The leg voltage references produced at this point are shown in Fig. 5 for comparison. Similarly, a comparison between the current waveforms at this operating point (Fig. 6 left) shows a larger current ripple produced by the double min-max injection compared to the second min-max injection. A higher ripple frequency can be observed by the current waveform produced under the second min-max injection. This leads to a lower current THD value under certain operating conditions. This is due to better centering of the active voltage vectors and equal distribution of the zero voltage vectors at the beginning and end of the modulation period with the second offset injection. At $m = 0.7$, the double and second min-max injections produce
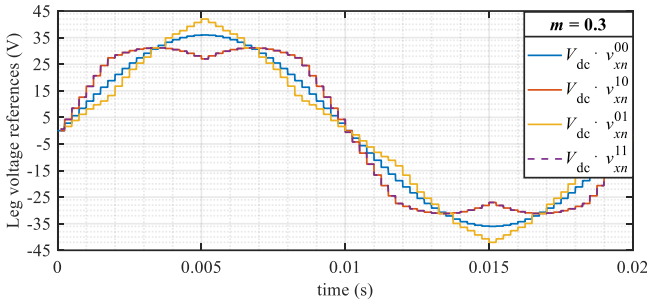
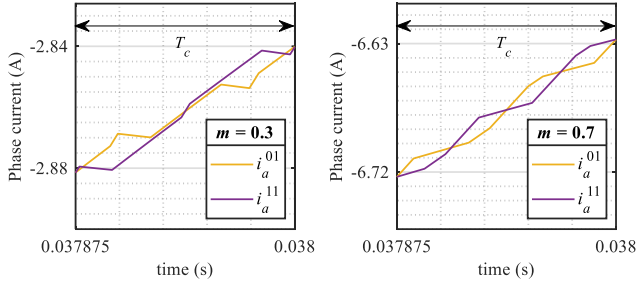Fig. 5   Leg voltage references under different injections ($m = 0.3$).

Fig. 6   Current ripple during same carrier interval ($T_c = 1/f_c$) for second and double min-max injections for $m = 0.3$ (left) and $m = 0.7$ (right).

similar THD values, and a comparison between the current waveforms at this point shows a similar ripple frequency (Fig. 6 right). Experimental verification of the simulation results is planned in the near future.

VI. CONCLUSION

It is well known that the space vector PWM becomes computationally intensive with an increase in the number of voltage levels and phases. Carrier-based methods with the first offset injection for two-level and double offset injection for multilevel converters are known to deliver performance comparable to the SVPWM, with superior resource utilization under IPD-PWM. However, in the case of a CHB multilevel converter under regular-sampled PWM, it has been observed that the double offset injection does not produce the best current THD for the linear modulation index range. Instead, new second (only) min-max injection is suggested which produces the best THD profile for modulation index range below unity. The double min-max injection ought to be used for the extension of the linear modulation range beyond unity with a better performance compared to the first offset injection. In terms of the multicarrier phase-shifted and level-shifted modulation strategies, IPD-PWM was found to produce the lowest harmonic distortion of the phase voltage and current waveforms throughout the linear modulation index range and is suggested to be used under a cyclic rotation of the carrier waveforms for even power distribution among battery-converter modules of a CHB.

REFERENCES

[1] J. Rodriguez, J. S. Lai, and F. Z. Peng, "Multilevel inverters: a survey of topologies, controls, and applications," IEEE Transactions on Industrial Electronics, vol. 49, no. 4, pp. 724-738, 2002.

[2] J. I. Leon, S. Vazquez, and L. G. Franquelo, "Multilevel converters: control and modulation techniques for their operation and industrial applications," Proceedings of the IEEE, vol. 105, no. 11, pp. 2066-2081, 2017.

[3] M. Malinowski, K. Gopakumar, J. Rodriguez, and M. A. Pérez, "A survey on cascaded multilevel inverters," IEEE Transactions on Industrial Electronics, vol. 57, no. 7, pp. 2197-2206, 2010.

[4] M. Malinowski, "Cascaded multilevel converters in recent research and applications," Bulletin of the Polish Academy of Sciences, vol. 65, no. 5, pp. 567-578, 2017.

[5] C. D. Townsend, T. J. Summers, and R. E. Betz, "Phase-shifted carrier modulation techniques for cascaded H-bridge multilevel converters," IEEE Transactions on Industrial Electronics, vol. 62, no. 11, pp. 6684-6696, 2015.

[6] J. S. Lai, and F. Z. Peng, "Multilevel converters-a new breed of power converters," IEEE Transactions on Industry Applications, vol. 32, no. 3, pp. 509-517, 1996.

[7] B. Mirafzal, "Survey of fault-tolerance techniques for three-phase voltage source inverters," IEEE Transactions on Industrial Electronics, vol. 61, no. 10, pp. 5192-5202, 2014.

[8] S. Farzamkia, H. Iman-Eini, A. Khoshkbar-Sadigh, M. Khaleghi, and M. Noushak, "Comparative and quantitative analyze on reliability of MMC-based and CHB-based drive systems considering various redundancy strategies," in 11th Power Electronics, Drive Systems, and Technologies Conference (PEDSTC), 2020, pp. 1-6.

[9] X. Shen, H. Lin, B. Li, J. Liu, J. I. Leon, L. Wu, and L. G. Franquelo, "Loss evaluation of cascaded H-bridge and modular multilevel converter for motor drive applications," in IECON 2018 - 44th Annual Conference of the IEEE Industrial Electronics Society, 2018, pp. 1299-1304.

[10] A. Marzoughi, R. Burgos, D. Boroyevich, and Y. Xue, "Design and comparison of cascaded H-bridge, modular multilevel converter, and 5-L active neutral point clamped topologies for motor drive applications," IEEE Transactions on Industry Applications, vol. 54, no. 2, pp. 1404-1413, 2018.

[11] L. G. Franquelo, J. Rodriguez, J. I. Leon, S. Kouro, R. Portillo, and M. A. M. Prats, "The age of multilevel converters arrives," IEEE Industrial Electronics Magazine, vol. 2, no. 2, pp. 28-39, 2008.

[12] D. G. Holmes, "The general relationship between regular-sampled pulse-width-modulation and space vector modulation for hard switched converters," in Conference Record of the 1992 IEEE Industry Applications Society Annual Meeting, 1992, pp. 1002-1009

[13] B. P. McGrath, D. G. Holmes, and T. Lipo, "Optimized space vector switching sequences for multilevel inverters," IEEE Transactions on Power Electronics, vol. 18, no. 6, pp. 1293-1301, 2003.

[14] W. Fei, "Sine-triangle versus space-vector modulation for three-level PWM voltage-source inverters," IEEE Transactions on Industry Applications, vol. 38, no. 2, pp. 500-506, 2002.

[15] D. G. Holmes, and T. A. Lipo, Pulse width modulation for power converters: principles and practice: John Wiley & Sons, 2003.

[16] Y. Cho, T. LaBella, J. Lai, and M. K. Senesky, "A carrier-based neutral voltage modulation strategy for multilevel cascaded inverters under unbalanced dc sources," IEEE Transactions on Industrial Electronics, vol. 61, no. 2, pp. 625-636, 2014.

[17] B. Xiao, L. Hang, J. Mei, C. Riley, L. M. Tolbert, and B. Ozpineci, "Modular cascaded H-bridge multilevel PV inverter with distributed MPPT for grid-connected applications," IEEE Transactions on Industry Applications, vol. 51, no. 2, pp. 1722-1731, 2015.

[18] Y. Hu, X. Zhang, W. Mao, T. Zhao, F. Wang, and Z. Dai, "An optimized third harmonic injection method for reducing dc-link voltage fluctuation and alleviating power imbalance of three-phase cascaded H-bridge photovoltaic inverter," IEEE Transactions on Industrial Electronics, vol. 67, no. 4, pp. 2488-2498, 2020.

[19] Y. Yu, G. Konstantinou, B. Hredzak, and V. G. Agelidis, "Power balance of cascaded H-bridge multilevel converters for large-scale photovoltaic integration," IEEE Transactions on Power Electronics, vol. 31, no. 1, pp. 292-303, 2016.

[20] O. Dordevic, M. Jones, and E. Levi, "A comparison of carrier-based and space vector PWM techniques for three-level five-phase voltage source inverters," IEEE Transactions on Industrial Informatics, vol. 9, no. 2, pp. 609-619, 2013.

[21] Ó. Lopez, J. Álvarez, A. G. Yepes, F. Baneira, D. Pérez-Estévez, F. D. Freijedo, and J. Doval-Gandoy, "Carrier-based PWM equivalent to multilevel multiphase space vector PWM techniques," IEEE Transactions on Industrial Electronics, vol. 67, no. 7, pp. 5220-5231, 2020.

[22] D. G. Holmes, "The significance of zero space vector placement for carrier-based PWM schemes," IEEE Transactions on Industry Applications, vol. 32, no. 5, pp. 1122-1129, 1996.